



## OPEN ACCESS

## EDITED BY

Kang Cui,  
University of Jinan, China

## REVIEWED BY

Tian Qiang,  
Jiangnan University, China  
Shipeng Zhang,  
Kwangwoon University, Republic of  
Korea  
Yanan Ding,  
Shandong University of Science and  
Technology, China

## \*CORRESPONDENCE

Qihui Zhou,  
✉ qihuizhou@uor.edu.cn  
Yuanyue Li,  
✉ yyli@qdu.edu.cn  
Zhao Yao,  
✉ yzh17@qdu.edu.cn

†These authors have contributed equally  
to this work

RECEIVED 27 September 2023

ACCEPTED 30 October 2023

PUBLISHED 09 November 2023

## CITATION

Lv L, Liu T, Jiang T, Li J, Zhang J, Zhou Q,  
Dhakal R, Li X, Li Y and Yao Z (2023), A  
highly sensitive flexible capacitive  
pressure sensor with hierarchical pyramid  
micro-structured PDMS-based dielectric  
layer for health monitoring.  
*Front. Bioeng. Biotechnol.* 11:1303142.  
doi: 10.3389/fbioe.2023.1303142

## COPYRIGHT

© 2023 Lv, Liu, Jiang, Li, Zhang, Zhou,  
Dhakal, Li, Li and Yao. This is an open-  
access article distributed under the terms  
of the [Creative Commons Attribution  
License \(CC BY\)](https://creativecommons.org/licenses/by/4.0/). The use, distribution or  
reproduction in other forums is  
permitted, provided the original author(s)  
and the copyright owner(s) are credited  
and that the original publication in this  
journal is cited, in accordance with  
accepted academic practice. No use,  
distribution or reproduction is permitted  
which does not comply with these terms.

# A highly sensitive flexible capacitive pressure sensor with hierarchical pyramid micro-structured PDMS-based dielectric layer for health monitoring

Luyu Lv<sup>1,2†</sup>, Tianxiang Liu<sup>1,2†</sup>, Ting Jiang<sup>1</sup>, Jiamin Li<sup>1,2</sup>, Jie Zhang<sup>1,2</sup>,  
Qihui Zhou<sup>1,3\*</sup>, Rajendra Dhakal<sup>4</sup>, Xiao Li<sup>5</sup>, Yuanyue Li<sup>2\*</sup> and  
Zhao Yao<sup>1,2\*</sup>

<sup>1</sup>Heart Center, Qingdao Hiser Hospital Affiliated of Qingdao University (Qingdao Traditional Chinese Medicine Hospital), Qingdao University, Qingdao, China, <sup>2</sup>College of Electronics and Information, Qingdao University, Qingdao, China, <sup>3</sup>School of Rehabilitation Sciences and Engineering, University of Health and Rehabilitation Sciences, Qingdao, China, <sup>4</sup>Department of Computer Science and Engineering, Sejong University, Seoul, Republic of Korea, <sup>5</sup>Hisense Visual Technology Co., Ltd., Qingdao, China

Herein, a flexible pressure sensor with high sensitivity was created using a dielectric layer featuring a hierarchical pyramid microstructure, both in simulation and fabrication. The capacitive pressure sensor comprises a hierarchically arranged dielectric layer made of polydimethylsiloxane (PDMS) with pyramid microstructures, positioned between copper electrodes at the top and bottom. The achievement of superior sensing performance is highly contingent upon the thickness of the dielectric layer, as indicated by both empirical findings and finite-element analysis. Specifically, the capacitive pressure sensor, featuring a dielectric layer thickness of 0.5 mm, exhibits a remarkable sensitivity of 0.77 kPa<sup>-1</sup> within the pressure range below 1 kPa. It also demonstrates an impressive response time of 55 ms and recovery time of 42 ms, along with a low detection limit of 8 Pa. Furthermore, this sensor showcases exceptional stability and reproducibility with up to 1,000 cycles. Considering its exceptional achievements, the pressure sensor has been effectively utilized for monitoring physiological signals, sign language gestures, and vertical mechanical force exerted on objects. Additionally, a 5 × 5 sensor array was fabricated to accurately and precisely map the shape and position of objects. The pressure sensor with advanced performance shows broad potential in electronic skin applications.

## KEYWORDS

PDMS, capacitive pressure sensor, hierarchical pyramid microstructure, high sensing performance, physiological signals monitoring

## Introduction

The flexible pressure sensor serves as a core component for electronic skin (Guo et al., 2022; Zheng et al., 2022; Zhu et al., 2022), enabling the emulation of human skin's sensing mechanism and exhibiting promising potential in wearable device applications (Lin et al., 2020; Lee et al., 2021; Lyu et al., 2021), smart prosthetics (Tian et al., 2019; Khoshmanesh et al., 2021), health monitoring (Rocha et al., 2021; Wang et al., 2022; Han et al., 2022), and body motion detection (Xiong et al., 2020; Zhu et al., 2021), etc. The classification of pressure sensors can be based on five distinct sensing mechanisms: piezoresistivity (Ding et al., 2020; Wang et al., 2022b; Ji et al., 2022), capacitance (Li et al., 2020; Qin et al., 2021; Wang et al., 2022c; Duan et al., 2022), piezoelectricity (Wang et al., 2021; Luo et al., 2021; Yi et al., 2022), field-effect transistors (Shi et al., 2020; Cheng et al., 2023), and triboelectricity (Wang et al., 2021; Liu et al., 2021; Xu et al., 2022). Among them, the capacitive pressure sensor has garnered substantial research for the superiority of outstanding structural stability, rapid response time, minimal power consumption, and a compact circuit design. Similar to the conventional parallel-plate capacitor, capacitive pressure sensors typically employ a "sandwich" structure, comprising a dielectric layer sandwiched between two electrodes positioned at the top and bottom. Its capacitance ( $C$ ) is determined by the dielectric layer's permittivity ( $\epsilon$ ), the effective area between two electrodes ( $A$ ), and the separation distance of plate electrodes ( $d$ ). Generally, the vertical force on the capacitive pressure sensor can induce variations in the dielectric layer thickness, leading to corresponding changes in the capacitance measurement. Therefore, it's vital to select a suitable material and optimize the structure configuration for the dielectric layer. Furthermore, the preparation of capacitive pressure sensors with controllable morphology on a large scale poses a significant challenge in achieving high performance.

The commonly utilized materials for fabricating the flexible dielectric layer include elastomers like polydimethylsiloxane (PDMS) (Wan et al., 2018; Hwang et al., 2021), polystyrene (Tian et al., 2020; Su et al., 2021), polyurethane (PU) (Seyedin et al., 2020; Zhu et al., 2020), etc. Among them, PDMS has emerged as the dominant choice for the dielectric layer owing to its reduced Young's modulus, enhanced thermal stability and improved chemical stability. Moreover, the implementation of the micro-structured designs on the dielectric layer, such as micro-pyramid (Yang et al., 2019; Li et al., 2020; Zhang et al., 2021; Tao et al., 2022), micro-porous (Li et al., 2020; He et al., 2020), micro-sphere (Jung et al., 2020; Xiong et al., 2020), micro-pillar (Luo et al., 2019; Cao et al., 2020), micro-wrinkles (Zeng et al., 2019; Tang et al., 2021), etc., has demonstrated its efficacy in enhancing sensor performance. Generally, the realization of the microstructure is based on the template replication approach, which consists of soft-lithography and hard-lithography. Soft-lithography technique exploits bionic micro-patterns to make microstructures via directly copying the morphology of natural substances. Wan et al. developed an exceptional sensitivity ( $1.2 \text{ kPa}^{-1}$ ) flexible tactile sensor by utilizing lotus leaf as template to obtain bionic microtowers array structure on PDMS substrate (Wan et al., 2018). Jian and colleagues developed pressure sensors that exhibit exceptional performance, featuring an impressive sensitivity of  $19.8 \text{ kPa}^{-1}$  and an incredibly low detection threshold of  $0.6 \text{ Pa}$ . These sensors were constructed

using a highly conductive active film combined with a bionic hierarchical microstructured PDMS substrate, which was replicated from the leaves of *E. aureum* plant species (Jian et al., 2017). However, it is difficult for large-scale fabrication. In addition, it suffers from an inherent flaw where the microstructure's shape, dimension, and spacing remain unalterable. Therefore, it is not feasible to fabricate structured micro-patterns with a predetermined form and dimension. The hard-lithography is an effective approach that can tackle the above problems. The hard-lithography depends on photolithography technique and wet etching to fabricate a patterned template that can be transferred to a flexible polymer material. Luo et al. have successfully designed a capacitive sensor utilizing a tilted pillar array dielectric layer, showcasing exceptional sensitivity of  $0.42 \text{ kPa}^{-1}$  below  $1 \text{ kPa}$ . The dielectric layer was molded from the tilted micro-structured template made by photolithography (Luo et al., 2019). In the same way, Tao and colleagues produced a novel dielectric layer using ionic gels with pyramidal-shaped microstructured to obtain an unprecedented sensitivity of  $41 \text{ kPa}^{-1}$  (Tao et al., 2022). Thanks to the implementation of a porous pyramid dielectric layer, Yang's group prepared an ultrahigh sensitive ( $44.5 \text{ kPa}^{-1}$ ) capacitive pressure sensor, which was designed to be unaffected by strain and temperature (Yang et al., 2019). The manufacturing process has merits of high precision, controllable aspect ratio, and mass production. Therefore, the hard-lithography technique enables the production of a microstructure that not only facilitates the efficient manufacturing of pressure sensors with superior performance on a large scale but also fulfills the requirement for convenient alteration of the microstructure's morphology.

In this research, an efficient hard-lithography technique was employed to fabricate an exceptional sensitivity capacitive pressure sensor. The sensor utilized copper foils for both the bottom and top electrodes, along with a PDMS dielectric layer that incorporates a hierarchical pyramid microstructure. The prepared flexible capacitive pressure sensor exhibits a remarkable sensitivity of  $0.77 \text{ kPa}^{-1}$  below  $1 \text{ kPa}$ . It also demonstrates an impressive response time of  $55 \text{ ms}$  and recovery time of  $42 \text{ ms}$ , along with a low detection limit of  $8 \text{ Pa}$ . Furthermore, this sensor showcases exceptional stability and reproducibility with up to  $1,000$  cycles. Moreover, the comparison was conducted to evaluate the impact of dielectric layer's microstructure and thickness on capacitive pressure sensors' sensitivity. Meanwhile, the sensing performance was further evaluated through finite element analysis (FEA) to investigate the impact of dielectric layer's microstructure and thickness. The increased deformation of the sensor with microstructure and thinner dielectric layer under identical pressure is responsible for this phenomenon. The development of a  $5 \times 5$  sensor array was undertaken to facilitate the identification of spatial pressure allocation exerted by various objects. Ultimately, the artificially created pressure sensor exhibits a vast array of potential applications, encompassing monitoring human biological signals, detecting body motion and vertical mechanical pressure.

## Experimental section

### Preparation process of a patterned silicon template

The patterned template was fabricated through the utilization of photolithography on  $<100>$  silicon wafers that were covered with a

300 nm thermally grown oxide layer. The processes involved in photolithography can be described follows (Ruth et al., 2020). Firstly, the silicon wafer underwent a cleaning process using acetone/IPA/DI water, followed by drying with N<sub>2</sub> blowing. Secondly, the silicon wafer's surface was spin-coated with the photoresist (KXN5735-L0 negative photoresist) at 500 rpm for 6 s and a subsequent coating at 3,000 rpm for 20 s. The photoresist film was subjected to a preliminary baking process at 100°C for 90 s and exposed by the UV aligner. The wafer backed again at 120°C for 90 s. Thirdly, the photoresist film was developed by TMAH (2.38%) for 30 s and post-baked at 120°C for 3 min before wet etching. Next, the silicon oxide layer was etched by buffer oxide etchant (BOE) for 5 min. Eventually, the special hierarchical pyramid microstructure of the silicon template was fabricated by anisotropic etching using 5 M KOH solution for 5 h.

## Fabrication process of a pressure sensor with hierarchical pyramid microstructure

Firstly, the PDMS and the curing agent were meticulously mixed in a 10:1 weight ratio. Secondly, after a 30-min treatment in the vacuum chamber, the mixture's bubbles were entirely eliminated. The mixture was introduced into the silicon template and subjected to spin-coating at a speed of 1,000 rpm, then cured at a temperature of 85°C for a duration of 1.5 h. It is important to mention that the spin-coating rate during the same period has an impact on the thickness of the dielectric layer. The dielectric layer was subsequently removed from the silicon template featuring a hierarchical pyramid microstructure. Ultimately, a flexible pressure sensor was developed by integrating a dielectric layer featuring hierarchical pyramid microstructures with copper foils as the upper and lower electrodes.

## Fabrication of a 5 × 5 sensor array

Five strips of copper foil with dimensions of 5 mm × 80 mm were applied to the polyimide (PI) tape in parallel at 5 mm intervals as the bottom electrode array. The identical procedure was employed to fabricate the top electrode array. The dielectric layer was fabricated using template replication technique, featuring a hierarchical pyramid microstructure. Once prepared, it was equally divided into 25 portions, each measuring 5 mm × 5 mm. The dielectric layer was securely adhered to the bottom electrode strips, while the top electrode strips were arranged orthogonally to form a 5 × 5 capacitive pressure sensor arrays (Ren et al., 2022).

## Measurement of sensing performance

The artificially created sensor was setup on the pressure gage (ZQ-990, Zhiqu) test platform, while its upper and lower electrodes were linked to the precision LCR meter (E4980, Keysight). The capacitive response was measured by applying varying force, utilizing a precision LCR meter with 100 kHz, 1 V bias. A USB connection was established between the LCR meter, ZQ-990, and a laptop for the purpose of post-processing and analyzing data. The

surface morphologies of the patterned silicon template and the prepared PDMS film were scanned using field-emission scanning electron microscopy (FESEM, Hitachi S-4800, Japan) to obtain high-resolution images.

# Results and discussion

## Fabrication and characterization

The flowchart of the photolithography process for the patterned silicon template are shown in Figure 1A. The fabrication process of the capacitive pressure sensor with the hierarchical pyramid microstructure dielectric layer is depicted in Figure 1B. The experiment setup for the sensing performance measurement is illustrated in Figure 1C. The Experimental Section provides a detailed account of the fabrication techniques employed and the methodology used for measuring the sensing performance. The SEM images of the patterned silicon template and the micro-structured PDMS film are depicted in Figure 2. The top view of the patterned silicon template reveals variations in microstructure size (Figure 2A), resulting in a visually striking hierarchical pyramid appearance. The distribution of these pyramids on the template exhibits a higher central peak and lower side peaks. The base of the pyramid is either a square or a rectangle in shape. The base of the pyramid exhibits a size variation ranging from approximately 40 μm–500 μm, while its height spans between 28 μm and 350 μm. After the templating process, the PDMS films display hierarchical pyramid microstructures as shown in Figure 2B.

## Pressure sensing performance of the flexible capacitive pressure sensor

The capacitive pressure sensor operates on the principle that its capacitive sensitive element converts the pressure signal into an electrical signal output that is directly proportional to the applied pressure. Similar to the conventional parallel-plate capacitor, the capacitive pressure sensor employs a “sandwich” structure, comprising a dielectric layer sandwiched between two electrodes positioned at the top and bottom (Li et al., 2018). Its capacitance  $C$  is determined by the equation:

$$C = \frac{\epsilon_0 \epsilon_r A}{d} \quad (1)$$

where  $\epsilon_0$  and  $\epsilon_r$  denote the dielectric constants of the vacuum and the dielectric layer. When a perpendicular pressure is exerted on the sensor, there will be a change in  $d$ , resulting in a modification of  $C$ . Conversely,  $A$  undergoes alteration when subjected to shear force (Zhao et al., 2015).

By optimizing the microstructures of the dielectric layer (Cao et al., 2020; Tao et al., 2022), incorporating silver nanowires into the dielectric layer (Fu et al., 2022), or distributing nanoparticles on the surface of the dielectric layer, significant enhancements can be achieved in terms of sensitivity for capacitive pressure sensors (Kim et al., 2018). The sensitivity in the first case is attributed to a reduction in  $d$ , while in the latter case it is due to an increase in  $\epsilon_r$ . Incorporating microstructures into the dielectric layer significantly

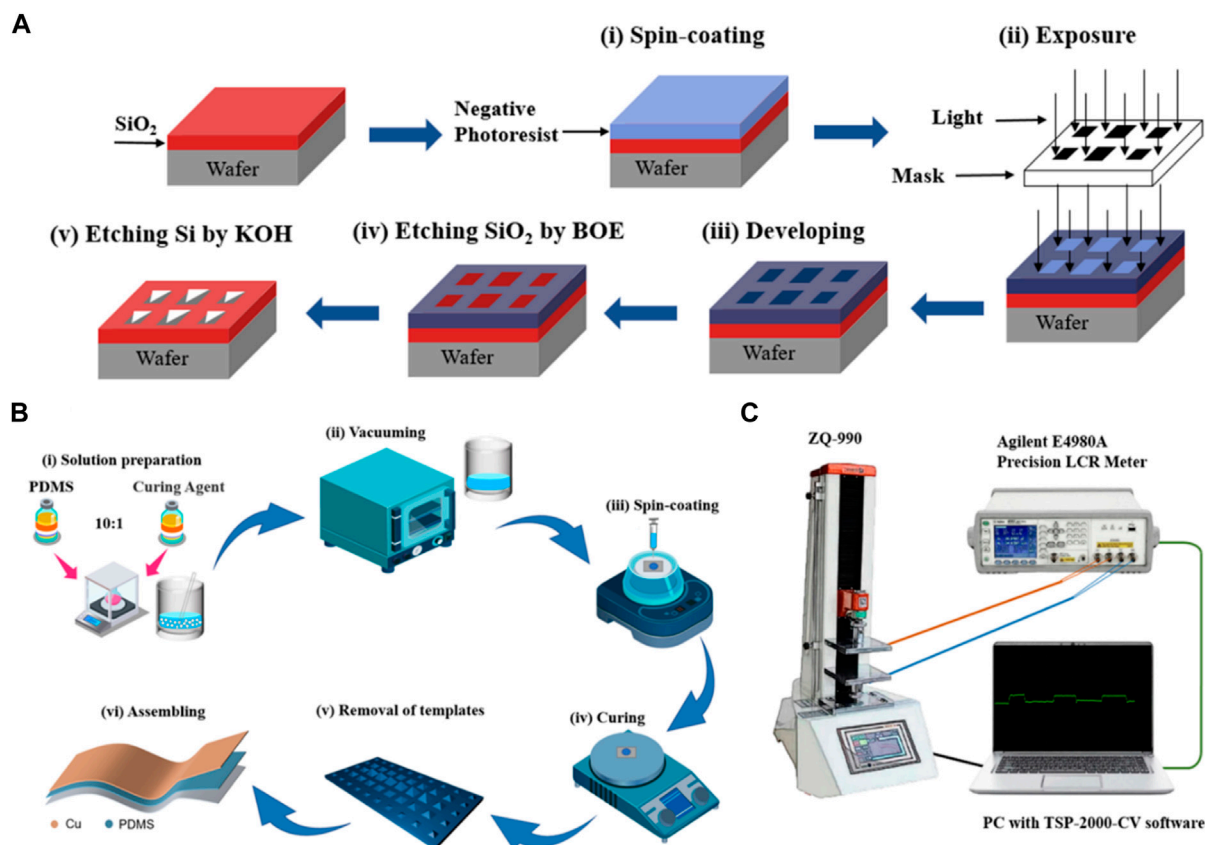


**FIGURE 1** (A) Flowchart of the photolithography process for the patterned silicon template. (B) Schematic representation of the fabrication process for the flexible capacitive pressure sensor. (C) Experiment setup for the sensing performance measurement.

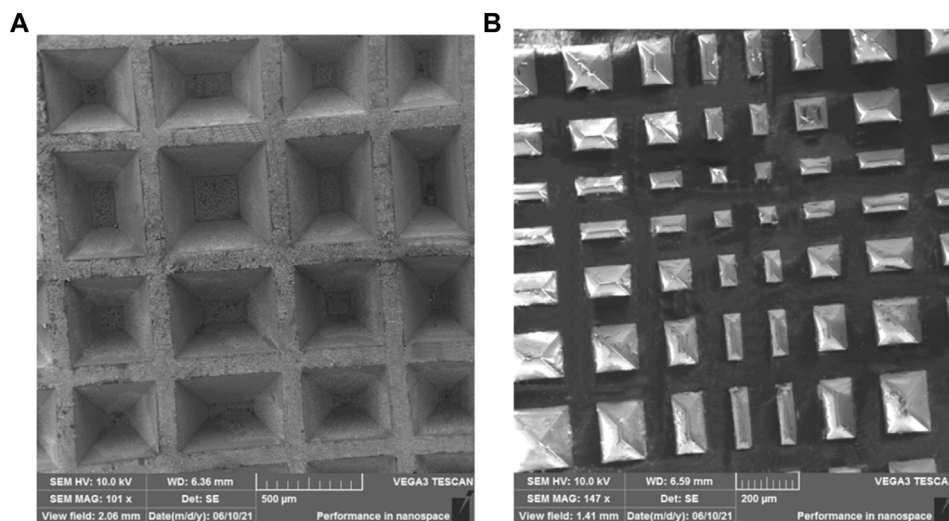


**FIGURE 2** (A) SEM image of the patterned silicon template. (B) SEM image of the pyramid-structured PDMS film.



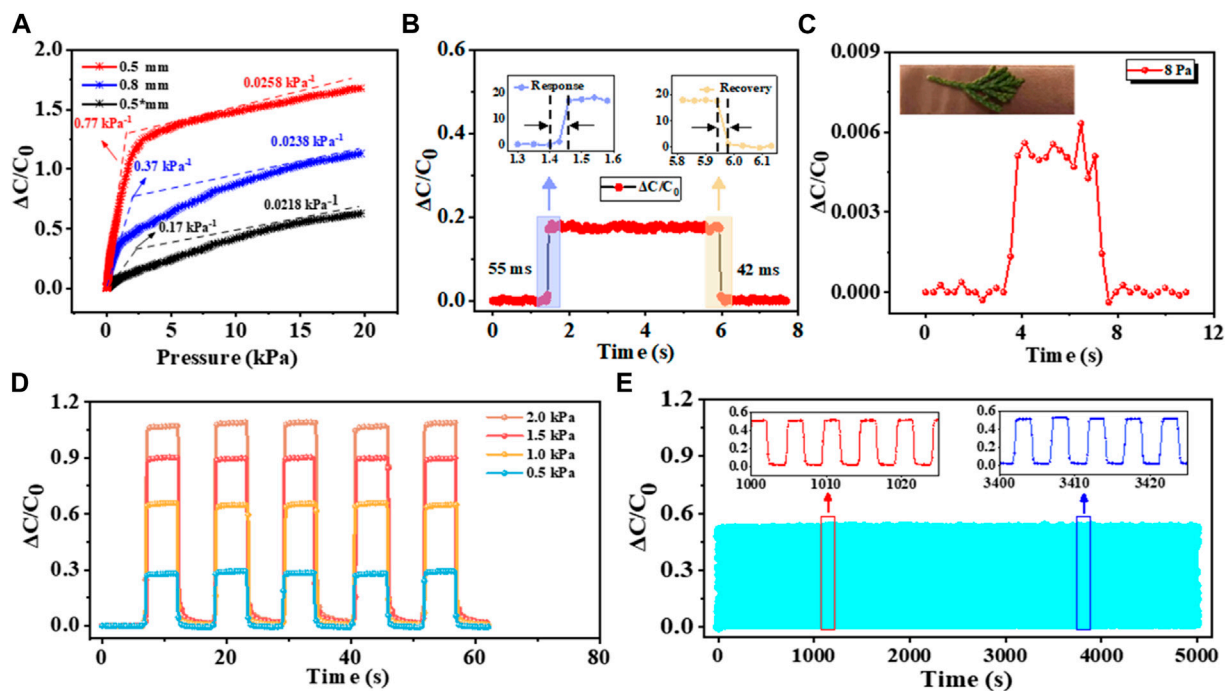


FIGURE 3

Sensing performance of the capacitive pressure sensor. (A) Sensitivity curves of capacitive pressure sensors based on the hierarchical pyramid microstructure dielectric layer with thicknesses of 0.5 mm (red) and 0.8 mm (blue), as well as the non-patterned dielectric layer with a thickness of 0.5 mm (black), respectively. (B) Real-time response under vertical pressure of  $\sim 400$  Pa (the insets show response and recovery time). (C) Capacitance response under a small pressure of  $\sim 8$  Pa. (D) Repeated real-time capacitance responses under 0.5, 1.0, 1.5, and 2.0 kPa. (E) 1,000 cycles for testing the stability of sensor under 0.8 kPa (the insets show the magnified view under different periods).

reduces its viscoelastic properties and greatly shortens both response and relaxation time. Based on the above discussion, a hierarchical pyramid microstructure dielectric layer has been designed. In comparison to other structures, this particular configuration enables greater deformation or higher change rate, resulting in rapid variations in capacitance and enhanced sensitivity.

The initial estimation of capacitive pressure sensor's fundamental sensing performance is conducted by applying vertical pressure. The evaluation of sensing performance heavily relies sensitivity ( $S$ ), which is commonly characterized as (Niu et al., 2020):

$$S = \frac{\delta(\Delta C/C_0)}{\delta P} \quad (2)$$

where  $C_0$  denotes the capacitance at the beginning and  $\Delta C$  represents difference in capacitance ( $C - C_0$ ), while  $P$  signifies the amount of vertical pressure exerted on the sensor. Based on the principle, the slope of the tangent of the pressure-capacitance curve reflects the level of sensitivity. As illustrated in Figure 3A, the variations in relative capacitance of the hierarchical pyramid microstructure sensor with the dielectric layer thickness of 0.5 mm was studied across a wide pressure range. To explore the impact of the dielectric layer's microstructure and thickness of on sensitivity, additional sensors with two different types of dielectric layers were produced for comparison: a planar dielectric layer measuring 0.5 mm in thickness and a hierarchical pyramid microstructure dielectric layer measuring 0.8 mm in thickness. As

shown in Figure 3A, the hierarchical pyramid microstructure pressure sensor with a dielectric layer thickness of 0.5 mm outperforms the other two instances. When the pressure is below 1 kPa, the hierarchical pyramid microstructure sensor with a dielectric layer thickness of 0.5 mm exhibits a sensitivity of  $0.77 \text{ kPa}^{-1}$ , which significantly surpasses the sensitivity ( $0.37 \text{ kPa}^{-1}$ ) of the sensor having a dielectric layer thickness of 0.8 mm. Conversely, the sensor featuring the planar dielectric layer demonstrates a comparatively lower sensitivity of  $0.17 \text{ kPa}^{-1}$ . When the pressure exceeds 1 kPa, there is a reduction in sensitivity for the aforementioned three sensors to  $0.0258 \text{ kPa}^{-1}$ ,  $0.0238 \text{ kPa}^{-1}$ , and  $0.0218 \text{ kPa}^{-1}$ , respectively. The exceptional sensitivity can be primarily attributed to the distinctive micro-pyramid architecture, as evidenced by the information provided earlier. Moreover, the correlation between the sensitivity and dielectric layer thickness becomes more evident as the dielectric layer thickness decreases from 0.8 mm to 0.5 mm, highlighting the impact of varying dielectric layer thickness on pressure sensor's sensitivity.

In addition to assessing sensitivity, an analysis on the response and recovery time measured by TSP-2000-CV was also performed. The sensor's capacitance quickly stabilizes within a mere 55 ms (top-left inset) when subjecting an object to a load of approximately 0.4 kPa, showcasing its exceptional response time, as illustrated in Figure 3B. After the elimination of the applied force, there is a rapid decline in the sensor's capacitance from its stable state to its initial value within a brief response period of 42 ms (top-right inset). It can be comparable to the human skin, typically ranging from 30 to

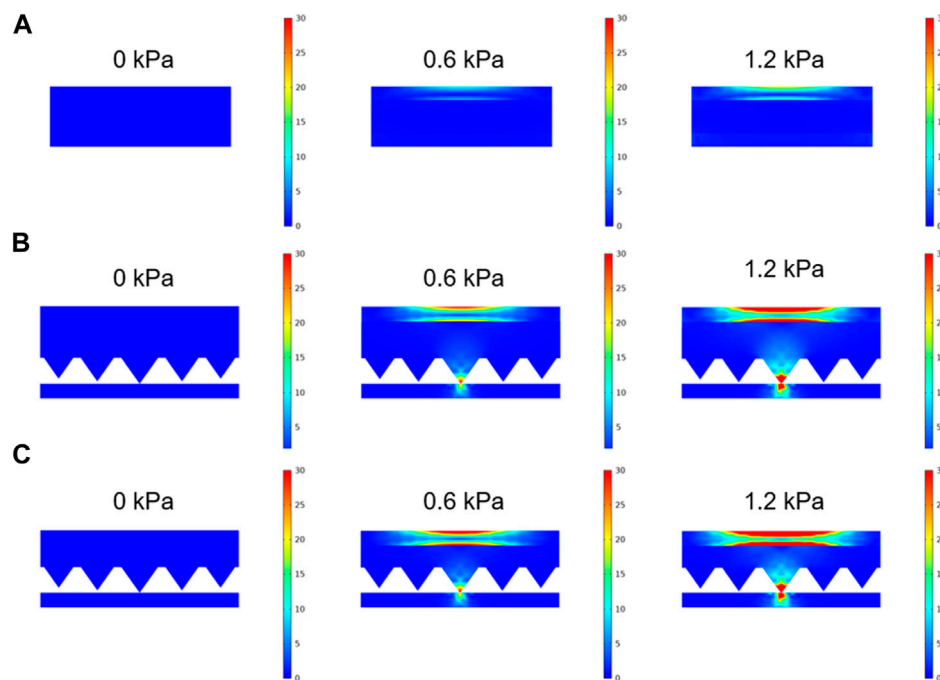


**FIGURE 4**

FEA simulation results of the pressure sensors. **(A)** Non-patterned sensor's contact stress distribution with a dielectric layer thickness measuring 0.5 mm under 0, 0.6, and 1.2 kPa, respectively. **(B)** Hierarchical pyramid microstructure sensor's contact stress distribution with a dielectric layer thickness of 0.8 mm under 0, 0.6, and 1.2 kPa, respectively. **(C)** Hierarchical pyramid microstructure sensor's contact stress distribution with the dielectric layer thickness of 0.5 mm under 0, 0.6, and 1.2 kPa, respectively.

50 ms. Such remarkable accomplishments can be ascribed to the PDMS's low viscoelasticity and the hierarchical pyramid microstructure. The capacitive pressure sensor is highly sensitive to detecting minute variations. With the assistance of the lightweight object ( $\sim 8$  Pa), the apparent alteration in capacitance during the loading/unloading process can be visible in Figure 3C. Its repeatability and discrimination capability under five repetitive exerting/releasing cycles with different vertical pressure is further assessed. The results in Figure 3D demonstrate real-time monitoring. By applied 0.5, 1.0, 1.5, and 2.0 kPa, respectively, the relative capacitance variation exhibits notable fluctuations while maintaining consistent levels under identical pressure condition. This suggests super repeatability and the ability to discern varying degrees of pressure. Moreover, given the paramount importance of long-term stability in practical applications, 1,000 loading/unloading cycles at 0.8 kPa were conducted to ensure its robustness. As shown in Figure 3E, the uniform waveforms devoid of discernible fatigue indicate that the sensor possesses prominent stability and reproducibility.

The sensing mechanism's validation was extended through FEA to examine the impact of dielectric layer's microstructure and thickness. The pressure sensors incorporated the dielectric layer configurations mentioned above were employed for comparative analysis. Figures 4A–C show the different stress distributions of the three sensors under 0, 0.6, and 1.2 kPa, respectively. As demonstrated in Figure 4A, under external vertical force, the whole contact surface of the planar sensor is deformed and the stress is distributed rather uniform. According to the parallel-plate capacitor definition, in this case, capacitance

change is primarily influenced by the separation distance due to infrequent variations in the contact area. Therefore, the sensitivity is extremely low as a result of the minimal variation in the distance between adjacent planes. However, for the hierarchical pyramid microstructure pressure sensor (Figure 4B, C), the concentration of force on the microstructure is enhanced under identical pressure, resulting in increased deformation of the dielectric layer. That will increase the contact area and decrease the gap simultaneously, ultimately resulting in the improvement of the sensitivity. Moreover, when subjected to identical pressure, the thin sensor demonstrates a more extensive distribution of contact stress compared to the thick sensor. Consequently, this leads to an increase deformation. In general, the hierarchical pyramid microstructure pressure sensor with a thin dielectric layer causes the highest sensitivity, aligning well with the experimental findings.

## Wearable applications of flexible capacitive pressure sensor

A pressure-sensitive device was attached to various points on the human body, including the wrist, elbow, and finger. Its purpose was to monitor physiological signals and track bodily movements including pulse rate, bending of the elbow, flexing of fingers, and twisting of the wrist, respectively. The pulse signals are crucial physiological indicators of an individual's health status. To identify wrist pulse, the pressure sensor has adhered to the participant's wrist and the resulting signals were showcased in Figure 5A. The

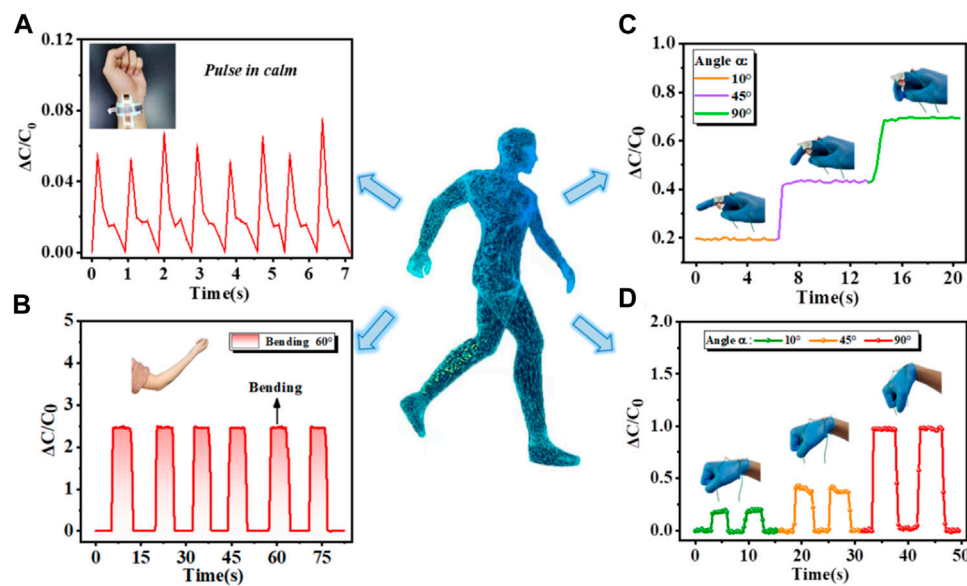


**FIGURE 5**

Various applications in recognition of physiological signals and human body motions. Real-time capacitance responses of different body positions including monitoring (A) wrist pulse under steady breath, (B) elbow with a bending angle of 60°, (C) finger, and (D) wrist with bending angles of 10°, 45°, and 90°, respectively.

displayed data and replicable pulse patterns, with a frequency of approximately 1 Hz that closely resembles that of a human wrist pulse. Hence, the sensor encouraging prospects in the surveillance of feeble biomedical signals. Besides, capacitance responses of the elbow bending are shown in Figure 5B. When the elbow undergoes flexion from a state of relaxation to an angle of 60°, there is a rapid and significant increase in the relative change in capacitance by up to 250%, which then stabilizes. Conversely, when the elbow is extended, there is a prompt decrease in the relative capacitance change from 250% to 0%. Then volunteer repeats the above steps and the uniform waveforms are obtained. It is indicated that the sensor demonstrates a swift response/recovery time and excellent stability in the presence of external force. Finally, the sensor's sensing performance is further assessed by placing it on the index finger and wrist while examining its response to various bending conditions. The initial position of the finger is set at a flexion angle of 10°, followed by subsequent adjustments to angles of 45° and 90°. It is evident from Figure 5C that the corresponding relative capacitance changes are ~20%, ~45%, and ~70%, respectively. The test results manifest a close correlation between the flexion angle and the proportional alteration in capacitance. Similarly, the capacitance is gradually enhanced through a controlled flexion degree of the wrist, enabling precise recognition of distinct bending movements, as can be witnessed in Figure 5D. Hence, the proposed sensor has broad application prospects in sign language gesture recognition. All of this information can be gathered in order to create a database for sign language, which will greatly facilitate the online teaching of sign language, autonomous learning, and other applications. In conclusion, the proposed sensor exhibits precise responsiveness to various repetitive dynamic flexion and extension motions and show repeatable reactions and relaxation behaviors in each cycle. The flexible pressure sensor holds potential for

functioning as a wearable sensor affixed to the skin, enabling the monitoring of human movements.

## Applications in vertical mechanical pressure

The pressure sensor also shows superior sensing performance in detecting vertical physical signals. The sensor was firstly mounted on the button of the remote control and constant continuous pressure is applied. The sensor's response to pressure is illustrated in Figure 6A, showing its rapid and stable characteristics. Subsequently, upon force removal, Figure 6B demonstrates a prompt reduction in relative capacitance change. Furthermore, the sensor was attached to phone screen and Figure 6C displays the synchronous and stable capacitance curves as a result of applying three sets of distinct forces repeatedly on the sensor. Due to its excellent mechanical stability and remarkable sensitivity, this technology offers a promising solution for addressing touch screen malfunctions. Finally, the sensor was attached to the sidewall of the paper cup, which was filled with different volumes of water. The relative capacitance change is relatively small when grabbing the paper cup containing a small amount of water, as illustrated in Figure 6D. As the quantity of water increases, relative capacitance change will enlarge significantly. Besides, the relative capacitance alteration remains consistent during two iterations of grasping or releasing the paper cup. It is the special micro-pyramid structure of the pressure sensor that makes it has high sensitivity and good stability. These findings demonstrate that the suggested sensor can alleviate the human condition of tactile sensory disorder and also be applied to robot tactile perception (Chen et al., 2023; Liu et al., 2023; Zhen et al., 2023).

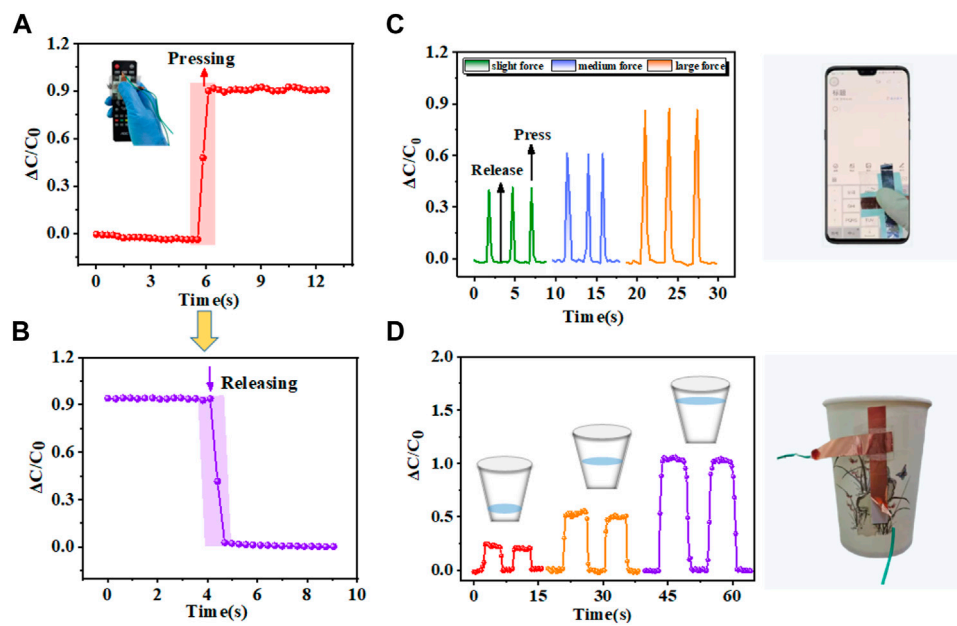


**FIGURE 6** Applications in vertical mechanical pressure. (A) Capacitance response upon pressing the button on the remote control. (B) Capacitance response upon releasing the button on the remote control. (C) Variations in relative capacitance of sensor on phone screen pressed with different forces. (D) Variations in relative capacitance positioned on the lateral surface of the paper cup while handling paper cups of varying weights.

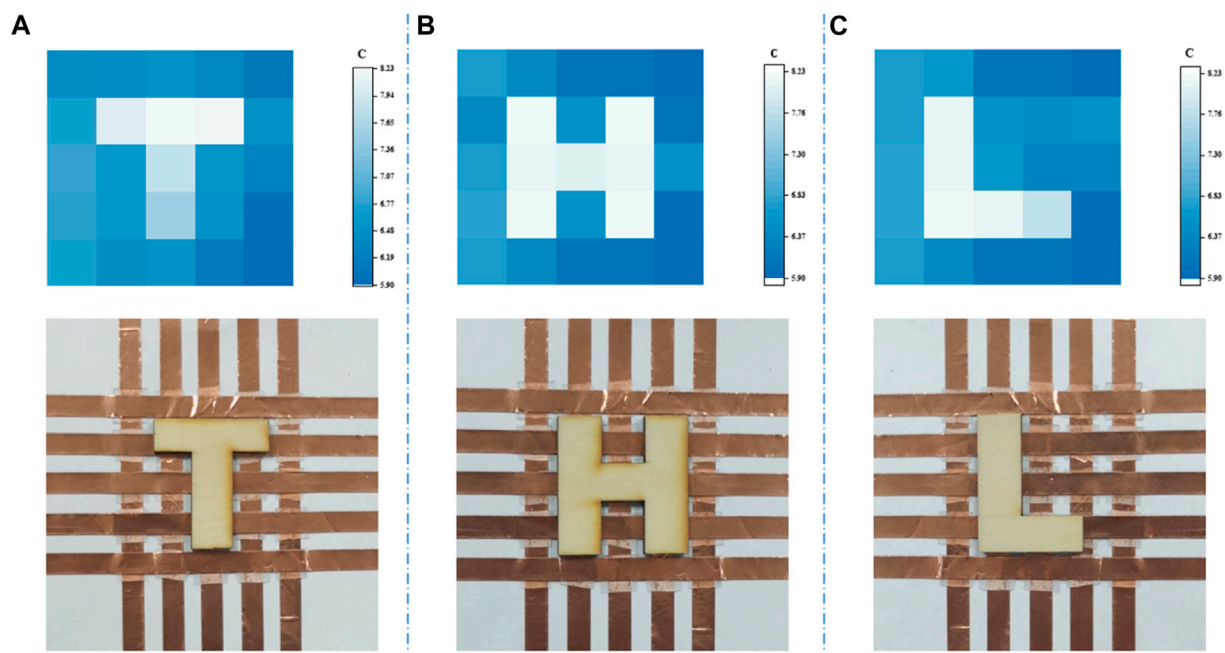


**FIGURE 7** Spatial pressure allocation images of the  $5 \times 5$  sensor array when loading wooden planks that are formed like the characters (A) "T", (B) "H", and (C) "L".

### Pressure mapping of sensor array

A significant drawback of a solitary pressure sensor is its inherent limitation in furnishing comprehensive data. To enhance

the applicability in practical scenarios, a  $5 \times 5$  multipixel of the pressure sensor array was integrated to form a sensor array measuring  $5 \times 5 \text{ cm}^2$ , in which each pressure sensor measures  $5 \times 5 \text{ mm}^2$ . When the sensor array's surface was covered by



wooden boards bearing the shapes of “T”, “H”, and “L”, their spatial distributions of the sensing response are shown in Figure 7. A noticeable contrast can be observed in the sensing response of the area that has been pressed and the one that has not. Meanwhile, the bright spot in the spatial pressure distribution image resembles the shape of a wooden board quite well, offering an efficient alternative in the wearable electronic device and flexible robot.

## Conclusion

In brief, an exceptionally sensitive and highly morphology-controllable flexible capacitive pressure sensor based on the hierarchical pyramid microstructure dielectric layer was successfully developed using an efficient strategy for pattern transfer of the silicon template. The hierarchically micro-pyramid structure's distinctive design facilitates outstanding sensing performances through efficient stress concentration. The prepared flexible capacitive pressure sensor exhibits a remarkable sensitivity of  $0.77 \text{ kPa}^{-1}$  below 1 kPa. It also demonstrates an impressive response time of 55 ms and recovery time of 42 ms, along with a low detection limit of 8 Pa. Furthermore, this sensor showcases exceptional stability and reproducibility with up to 1,000 cycles. According to the findings from both experimental results and FEA simulations, it can be concluded that the sensing performance is significantly influenced by the thickness of the dielectric layer. The fabricated pressure sensor possesses the ability to continuously monitor pulse signals on the wrist and tracking human body movements in real-time. What is even more significant, an advanced  $5 \times 5$  sensor array has been undertaken to demonstrate its capability in discerning different objects' spatial pressure distribution. It is surely believed that the hierarchical pyramid microstructure by the silicon template-assisted manufacturing strategy can spark fresh ideas for advancing flexible pressure sensor technology and will pave the way for various applications including intelligent robotics, biomedical monitoring, smart prosthetics as well as disease prevention and diagnostics.

## Data availability statement

The raw data supporting the conclusion of this article will be made available by the authors, without undue reservation.

## References

- Cao, Z., He, K., Xiong, W., Chen, Y., Qiu, X., Yu, D., et al. (2020). Flexible micropillar array for pressure sensing in high density using image sensor. *Adv. Mater. Inter* 7, 1902205. doi:10.1002/admi.201902205
- Chen, Y., Chernogor, L. F., Zheng, Y., Jin, Z., Sun, Z., Yao, Z., et al. (2023). Effect of remimazolam vs. propofol on hemodynamics during general anesthesia induction in elderly patients: single-center, randomized controlled trial. *IEEE Trans. Circuits Syst. II* 1, 10. doi:10.7555/JBR.37.20230110
- Cheng, G., Xu, H., Gao, N., Zhang, M., Gao, H., Sun, B., et al. (2023). Carbon nanotubes field-effect transistor pressure sensor based on three-dimensional conformal force-sensitive gate modulation. *Carbon* 204, 456–464. doi:10.1016/j.carbon.2022.12.090
- Ding, X., Zhong, W., Jiang, H., Li, M., Chen, Y., Lu, Y., et al. (2020). Highly accurate wearable piezoresistive sensors without tension disturbance based on weaved conductive yarn. *ACS Appl. Mat. Interfaces* 12, 35638–35646. doi:10.1021/acsami.0c07928

## Author contributions

LL: Data curation, Formal Analysis, Investigation, Methodology, Writing—original draft. TL: Data curation, Formal Analysis, Investigation, Methodology, Writing—original draft. TJ: Data curation, Writing—review and editing. JL: Writing—review and editing, Formal Analysis, Investigation. JZ: Investigation, Writing—review and editing, Data curation. QZ: Investigation, Writing—review and editing. RD: Writing—review and editing, Resources. XL: Writing—review and editing, Methodology. YL: Conceptualization, Funding acquisition, Project administration, Resources, Supervision, Writing—review and editing. ZY: Supervision, Writing—review and editing, Funding acquisition, Project administration, Resources.

## Funding

This work was supported in part by the National Natural Science Foundation of China under Grant 61904092, 62301291, and 6211101132, in part by the Youth Innovation Team Project of Shandong Provincial Education Department No. 2022KJ141, in part by the Shandong Provincial Natural Science Foundation of China under Grant ZR2021ME052, and in part by College Students Innovation and Entrepreneurship Training Program under Grant S202011065132.

## Conflict of interest

Author XL was employed by Hisense Visual Technology Co., Ltd.

The remaining authors declare that the research was conducted in the absence of any commercial or financial relationships that could be construed as a potential conflict of interest.

## Publisher's note

All claims expressed in this article are solely those of the authors and do not necessarily represent those of their affiliated organizations, or those of the publisher, the editors and the reviewers. Any product that may be evaluated in this article, or claim that may be made by its manufacturer, is not guaranteed or endorsed by the publisher.

- Duan, Y., Wu, J., He, S., Su, B., Li, Z., and Wang, Y. (2022). Bioinspired spinosum capacitive pressure sensor based on CNT/PDMS nanocomposites for broad range and high sensitivity. *Nanomaterials* 12, 3265. doi:10.3390/nano12193265

- Fu, D., Wang, R., Wang, Y., Sun, Q., Cheng, C., Guo, X., et al. (2022). An easily processable silver nanowires-dual-cellulose conductive paper for versatile flexible pressure sensors. *Carbohydr. Polym.* 283, 119135. doi:10.1016/j.carbpol.2022.119135

- Guo, Q., Qiu, X., and Zhang, X. (2022). Recent advances in electronic skins with multiple-stimuli-responsive and self-healing abilities. *Materials* 15, 1661. doi:10.3390/ma15051661

- Han, F., Wang, T., Liu, G., Liu, H., Xie, X., Wei, Z., et al. (2022). Materials with tunable optical properties for wearable epidermal sensing in health monitoring. *Adv. Mater.* 34, 2109055. doi:10.1002/adma.202109055

- He, Y., Zhao, L., Zhang, J., Liu, L., Liu, H., and Liu, L. (2020). A breathable, sensitive and wearable piezoresistive sensor based on hierarchical micro-porous PU@CNT films

- for long-term health monitoring. *Compos. Sci. Technol.* 200, 108419. doi:10.1016/j.compscitech.2020.108419
- Hwang, J., Kim, Y., Yang, H., and Oh, J. H. (2021). Fabrication of hierarchically porous structured PDMS composites and their application as a flexible capacitive pressure sensor. *Compos. Part B Eng.* 211, 108607. doi:10.1016/j.compositesb.2021.108607
- Ji, F., Sun, Z., Hang, T., Zheng, J., Li, X., Duan, G., et al. (2022). Flexible piezoresistive pressure sensors based on nanocellulose aerogels for human motion monitoring: a review. *Compos. Commun.* 35, 101351. doi:10.1016/j.coco.2022.101351
- Jian, M., Xia, K., Wang, Q., Yin, Z., Wang, H., Wang, C., et al. (2017). Flexible and highly sensitive pressure sensors based on bionic hierarchical structures. *Adv. Funct. Mater.* 27, 1606066. doi:10.1002/adfm.201606066
- Jung, Y., Lee, W., Jung, K., Park, B., Park, J., Ko, J., et al. (2020). A highly sensitive and flexible capacitive pressure sensor based on a porous three-dimensional PDMS/microsphere composite. *Polymers* 12, 1412. doi:10.3390/polym12061412
- Khosmanesh, F., Thurgood, P., Pirogova, E., Nahavandi, S., and Baratchi, S. (2021). Wearable sensors: at the frontier of personalised health monitoring, smart prosthetics and assistive technologies. *Biosens. Bioelectron.* 176, 112946. doi:10.1016/j.bios.2020.112946
- Kim, H., Kim, G., Kim, T., Lee, S., Kang, D., Hwang, M., et al. (2018). Transparent, flexible, conformal capacitive pressure sensors with nanoparticles. *Small* 14, 1703432. doi:10.1002/sml.201703432
- Lee, S., Kim, H., Park, M. J., and Jeon, H. J. (2021). Current advances in wearable devices and their sensors in patients with depression. *Front. Psychiatry* 12, 672347. doi:10.3389/fpsy.2021.672347
- Li, J., Bao, R., Tao, J., Peng, Y., and Pan, C. (2018). Recent progress in flexible pressure sensor arrays: from design to applications. *J. Mat. Chem. C* 6, 11878–11892. doi:10.1039/C8TC02946F
- Li, M., Liang, J., Wang, X., and Zhang, M. (2020a). Ultra-sensitive flexible pressure sensor based on microstructured electrode. *Sensors* 20, 371. doi:10.3390/s20020371
- Li, W., Jin, X., Zheng, Y., Chang, X., Wang, W., Lin, T., et al. (2020b). A porous and air gap elastomeric dielectric layer for wearable capacitive pressure sensor with high sensitivity and a wide detection range. *J. Mat. Chem. C* 8, 11468–11476. doi:10.1039/D0TC00443J
- Lin, J., Zhu, Z., Cheung, C. F., Yan, F., and Li, G. (2020). Digital manufacturing of functional materials for wearable electronics. *J. Mat. Chem. C* 8, 10587–10603. doi:10.1039/D0TC01112F
- Liu, L., Chen, H., Sun, H., Jin, Z., Chernogor, L. F., Batrakov, D. O., et al. (2023). A broadband circularly polarized antenna based on transparent conformal metasurface. *Antennas Wirel. Propag. Lett.*, 1–5. doi:10.1109/LAWP.2023.3316427
- Liu, S., Yuan, G., Zhang, Y., Xie, L., Shen, Q., Lei, H., et al. (2021). A self-powered gas sensor based on coupling triboelectric screening and impedance matching effects. *Adv. Mater. Technol.* 6, 2100310. doi:10.1002/admt.202100310
- Luo, J., Zhang, L., Wu, T., Song, H., and Tang, C. (2021). Flexible piezoelectric pressure sensor with high sensitivity for electronic skin using near-field electrohydrodynamic direct-writing method. *Extreme Mech. Lett.* 48, 101279. doi:10.1016/j.eml.2021.101279
- Luo, Y., Shao, J., Chen, S., Chen, X., Tian, H., Li, X., et al. (2019). Flexible capacitive pressure sensor enhanced by tilted micropillar arrays. *ACS Appl. Mat. Interfaces* 11, 17796–17803. doi:10.1021/acsami.9b03718
- Lyu, Q., Gong, S., Yin, J., Dyson, J. M., and Cheng, W. (2021). Soft wearable healthcare materials and devices. *Adv. Healthc. Mater.* 10, 2100577. doi:10.1002/adhm.202100577
- Niu, H., Gao, S., Yue, W., Li, Y., Zhou, W., and Liu, H. (2020). Highly morphology-controllable and highly sensitive capacitive tactile sensor based on epidermis-dermis-inspired interlocked asymmetric-nanocone arrays for detection of tiny pressure. *Small* 16, 1904774. doi:10.1002/sml.201904774
- Qin, R., Hu, M., Li, X., Liang, T., Tan, H., Liu, J., et al. (2021). A new strategy for the fabrication of a flexible and highly sensitive capacitive pressure sensor. *Microsyst. Nanoeng.* 7, 100. doi:10.1038/s41378-021-00327-1
- Ren, M., Sun, Z., Zhang, M., Yang, X., Guo, D., Dong, S., et al. (2022). A high-performance wearable pressure sensor based on an MXene/PVP composite nanofiber membrane for health monitoring. *Nanoscale Adv.* 4, 3987–3995. doi:10.1039/D2NA00339B
- Rocha, H., Semprinoschnig, C., and Nunes, J. P. (2021). Sensors for process and structural health monitoring of aerospace composites: a review. *Eng. Struct.* 237, 112231. doi:10.1016/j.engstruct.2021.112231
- Ruth, S. R. A., Beker, L., Tran, H., Feig, V. R., Matsuhisa, N., and Bao, Z. (2020). Rational design of capacitive pressure sensors based on pyramidal microstructures for specialized monitoring of biosignals. *Adv. Funct. Mater.* 30, 1903100. doi:10.1002/adfm.201903100
- Seyedin, S., Uzun, S., Levitt, A., Anasori, B., Dion, G., Gogotsi, Y., et al. (2020). MXene composite and coaxial fibers with high stretchability and conductivity for wearable strain sensing textiles. *Adv. Funct. Mater.* 30, 1910504. doi:10.1002/adfm.201910504
- Shi, W., Guo, Y., and Liu, Y. (2020). When flexible organic field-effect transistors meet biomimetics: a prospective view of the internet of things. *Adv. Mater.* 32, 1901493. doi:10.1002/adma.201901493
- Su, X., Luo, C., Yan, W., Jiao, J., and Zhong, D. (2021). Microdome-tunable graphene/carbon nanotubes pressure sensors based on polystyrene array for wearable electronics. *Materials* 14, 7385. doi:10.3390/ma14237385
- Tang, X., Yang, W., Yin, S., Tai, G., Su, M., Yang, J., et al. (2021). Controllable graphene wrinkle for a high-performance flexible pressure sensor. *ACS Appl. Mat. Interfaces* 13, 20448–20458. doi:10.1021/acsami.0c22784
- Tao, K., Chen, Z., Yu, J., Zeng, H., Wu, J., Wu, Z., et al. (2022). Ultra-sensitive, deformable, and transparent triboelectric tactile sensor based on micro-pyramid patterned ionic hydrogel for interactive human-machine interfaces. *Adv. Sci.* 9, 2104168. doi:10.1002/advs.202104168
- Tian, L., Zimmerman, B., Akhtar, A., Yu, K. J., Moore, M., Wu, J., et al. (2019). Large-area MRI-compatible epidermal electronic interfaces for prosthetic control and cognitive monitoring. *Nat. Biomed. Eng.* 3, 194–205. doi:10.1038/s41551-019-0347-x
- Tian, Q., Yan, W., Li, Y., and Ho, D. (2020). Bean pod-inspired ultrasensitive and self-healing pressure sensor based on laser-induced graphene and polystyrene microsphere sandwiched structure. *ACS Appl. Mat. Interfaces* 12, 9710–9717. doi:10.1021/acsami.9b18873
- Wan, Y., Qiu, Z., Hong, Y., Wang, Y., Zhang, J., Liu, Q., et al. (2018). A highly sensitive flexible capacitive tactile sensor with sparse and high-aspect-ratio microstructures. *Adv. Elect. Mater.* 4, 1700586. doi:10.1002/aelm.201700586
- Wang, H., Li, Z., Liu, Z., Fu, J., Shan, T., Yang, X., et al. (2022a). Flexible capacitive pressure sensors for wearable electronics. *J. Mat. Chem. C* 10, 1594–1605. doi:10.1039/D1TC05304C
- Wang, J., Cui, P., Zhang, J., Ge, Y., Liu, X., Xuan, N., et al. (2021a). A stretchable self-powered triboelectric tactile sensor with EGaN alloy electrode for ultra-low-pressure detection. *Nano Energy* 89, 106320. doi:10.1016/j.nanoen.2021.106320
- Wang, S., Shao, H.-Q., Liu, Y., Tang, C.-Y., Zhao, X., Ke, K., et al. (2021b). Boosting piezoelectric response of PVDF-TrFE via MXene for self-powered linear pressure sensor. *Compos. Sci. Technol.* 202, 108600. doi:10.1016/j.compscitech.2020.108600
- Wang, Y., Haick, H., Guo, S., Wang, C., Lee, S., Yokota, T., et al. (2022b). Skin bioelectronics towards long-term, continuous health monitoring. *Chem. Soc. Rev.* 51, 3759–3793. doi:10.1039/D2CS00207H
- Wang, Y., Yue, Y., Cheng, F., Cheng, Y., Ge, B., Liu, N., et al. (2022c). Ti<sub>3</sub>C<sub>2</sub>T<sub>x</sub> MXene-based flexible piezoresistive physical sensors. *ACS Nano* 16, 1734–1758. doi:10.1021/acsnano.1c09925
- Xiong, Y., Shen, Y., Tian, L., Hu, Y., Zhu, P., Sun, R., et al. (2020). A flexible, ultra-highly sensitive and stable capacitive pressure sensor with convex microarrays for motion and health monitoring. *Nano Energy* 70, 104436. doi:10.1016/j.nanoen.2019.104436
- Xu, R., Luo, F., Zhu, Z., Li, M., and Chen, B. (2022). Flexible wide-range triboelectric sensor for physiological signal monitoring and human motion recognition. *ACS Appl. Electron. Mat.* 4, 4051–4060. doi:10.1021/acsaem.2c00681
- Yang, J. C., Kim, J.-O., Oh, J., Kwon, S. Y., Sim, J. Y., Kim, D. W., et al. (2019). Microstructured porous pyramid-based ultrahigh sensitive pressure sensor insensitive to strain and temperature. *ACS Appl. Mat. Interfaces* 11, 19472–19480. doi:10.1021/acsami.9b03261
- Yi, Z., Liu, Z., Li, W., Ruan, T., Chen, X., Liu, J., et al. (2022). Piezoelectric dynamics of arterial pulse for wearable continuous blood pressure monitoring. *Adv. Mater.* 34, 2110291. doi:10.1002/adma.202110291
- Zeng, X., Wang, Z., Zhang, H., Yang, W., Xiang, L., Zhao, Z., et al. (2019). Tunable, ultrasensitive, and flexible pressure sensors based on wrinkled microstructures for electronic skins. *ACS Appl. Mat. Interfaces* 11, 21218–21226. doi:10.1021/acsami.9b02518
- Zhang, Z., Gui, X., Hu, Q., Yang, L., Yang, R., Huang, B., et al. (2021). Highly sensitive capacitive pressure sensor based on a micropillar array for health and motion monitoring. *Adv. Elect. Mater.* 7, 2100174. doi:10.1002/aelm.202100174
- Zhao, X., Hua, Q., Yu, R., Zhang, Y., and Pan, C. (2015). Flexible, stretchable and wearable multifunctional sensor array as artificial electronic skin for static and dynamic strain mapping. *Adv. Elect. Mater.* 1, 1500142. doi:10.1002/aelm.201500142
- Zhen, Q., Mao, Z., Cui, J., Guo, M., Chernogor, L. F., Jin, Z., et al. (2023). RCS reduction effect based on transparent and flexible polarization conversion metasurface arrays. *Results Phys.* 52, 106886. doi:10.1016/j.rinp.2023.106886
- Zheng, S., Li, W., Ren, Y., Liu, Z., Zou, X., Hu, Y., et al. (2022). Moisture-wicking, breathable, and intrinsically antibacterial electronic skin based on dual-gradient poly(ionic liquid) nanofiber membranes. *Adv. Mater.* 34, 2106570. doi:10.1002/adma.202106570
- Zhu, G.-J., Ren, P.-G., Wang, J., Duan, Q., Ren, F., Xia, W.-M., et al. (2020). A highly sensitive and broad-range pressure sensor based on polyurethane mesodome arrays embedded with silver nanowires. *ACS Appl. Mat. Interfaces* 12, 19988–19999. doi:10.1021/acsami.0c03697
- Zhu, M., Li, J., Yu, J., Li, Z., and Ding, B. (2022). Superstable and intrinsically self-healing fibrous membrane with bionic confined protective structure for breathable electronic skin. *Angew. Chem. Int. Ed.* 61, e202200226. doi:10.1002/anie.202200226
- Zhu, Y., Sun, F., Jia, C., Zhao, T., and Mao, Y. (2021). A stretchable and self-healing hybrid nano-generator for human motion monitoring. *Nanomaterials* 12, 104. doi:10.3390/nano12010104